



ELSEVIER

Available online at www.sciencedirect.com

Engineering Fracture Mechanics 75 (2008) 2385–2397

**Engineering
Fracture
Mechanics**

www.elsevier.com/locate/engfracmech

Interaction of dynamic mode-I cracks with inclined interfaces

V.B. Chalivendra ^{a,*}, A.J. Rosakis ^b

^a *Department of Mechanical Engineering, University of Massachusetts Dartmouth, 285 Old Westport Road, North Dartmouth, MA 02747, USA*

^b *Graduate Aeronautical Laboratories, California Institute of Technology, Pasadena, CA 91125, USA*

Received 15 February 2007; received in revised form 6 August 2007; accepted 7 August 2007

Available online 17 August 2007

Abstract

In this paper, we report on an experimental study of the deflection/penetration behavior of dynamic mode-I cracks propagating at two different crack velocities (slower and faster) toward inclined weak interfaces of three dissimilar angles (α): 30°, 45° and 60°. A simple wedge-loading specimen configuration as proposed by Xu et al. [Xu LR, Huang YY, Rosakis AJ. Dynamic crack deflection and penetration at interface in homogenous materials: experimental studies and model predictions. *J Mech Phys Solids* 2003;51:461–86], made of brittle Homalite-100, is used. A modified Hopkinson bar setup is used to achieve well-controlled impact loading conditions. Dynamic photoelasticity in conjunction with high-speed photography is used to capture real-time isochromatics associated with deflected/penetrated cracks.

© 2007 Elsevier Ltd. All rights reserved.

Keywords: Dynamic fracture; Inclined interfaces; Crack deflection and penetration; Dynamic photoelasticity; High-speed photography

1. Introduction

Cracks usually propagate in homogeneous, brittle solids under locally mode-I conditions, at sub-Rayleigh wave speeds (C_R) typically below the crack branching speed [1,2]. Even though the crack accelerates under increasing far-field loading, it reaches a critical speed beyond which it becomes energetically more favorable to propagate with multiple, branched crack tips rather than as a single entity. However if a crack is considered to propagate along a weak path, the weak path traps the crack, suppressing any tendency of branching or kinking out of the weak plane and permits very fast crack growth approaching the Rayleigh wave speed of the parent material [3,4]. However, when the mode-II cracks are made to propagate along such weak paths, they tend to go even faster, with speeds that are within the intersonic regime of the solid [4–6].

Literature reveals that extreme mode-I and mode-II cases have been studied both experimentally and theoretically. However, little has been reported about the dynamic mixed-mode crack growth along weak paths. Geubelle and Kubair [6] reported the transition of an incident mode-I crack into a mixed-mode crack as it

* Corresponding author. Tel.: +1 508 910 6572; fax: +1 508 999 8881.
E-mail address: vchalivendra@umassd.edu (V.B. Chalivendra).

come across a weak plane or interface. Xu and Rosakis [7] experimentally observed the transition of subsonic mode-I cracks after approaching the interface, propagating as shear-dominated interface cracks at intersonic speeds. Recently Xu et al. [8] also experimentally observed a speed jump or dramatic speed increase as the crack transitions from a purely mode-I crack to an unstable mixed-mode interfacial crack. In their paper, they compared experimental speed jump phenomenon with theoretical predictions based on energy criterion. They also discussed the deflection behavior of mode-I cracks (propagating in Homalite-100 material) upon reaching the inclined interfaces of various strengths and different inclined interface angles. It is appropriate to mention here that numerous research efforts have been reported on static deflection/penetration behavior at an interface in the past years for various kinds of materials [9–17].

This paper presents an extension of the experimental work reported by Xu et al. [8]. In their paper, they investigated only one case of incipient mode-I crack speed, which is slightly less than the critical or branching speed of Homalite-100 material ($0.35\text{--}0.4C_R$). In real-life situations, the materials are made out of several bonded substrates, as is the case with fiber reinforced composites, semiconductor materials, and layered materials in airplanes. As reported above, the cracks can propagate at much higher speeds approaching Rayleigh wave speeds along the weak planes or interfaces of these layered materials. Since interfaces are usually weaker than the constituent materials, their interface failure under dynamic loading conditions is the active failure mechanism in such solids [18]. Indeed any defects in such interfaces can ultimately serve as sites of catastrophic failure nucleation during the service life of the structure.

Motivated by the above real-life situations of layered materials, this experimental study is conducted to investigate the deflection/penetration behavior that occurs when an incipient mode-I crack propagating at a speed close to $0.8\text{--}0.9C_R$ approaches the inclined weak interface. The deflection/penetration behavior of faster mode-I cracks is also compared with that of slower cracks. The experiments in slower crack speed are repeated in this study for comparison purposes. Similar to Xu et al. [8], weakly bonded material systems composed of identical constituent solids are considered so that the resulting material remains constitutively homogeneous. However, the existence of weak bonds (bonds of lower fracture toughness) makes this material system inhomogeneous regarding its fracture toughness behavior. This avoids the complication of the material property and wave speed mismatch across the interface, while maintaining the essential properties of a weak path or bond whose strength can be experimentally varied. In contrast to the loading setup used by Xu et al. [8], a modified Hopkinson bar setup is used to have well-controlled dynamic loading of the specimen. The loading histories of each specimen are recorded using strain gages bonded onto the notch faces of the specimen. This facilitates proper comparison of the results of various specimen configurations with similar loading conditions.

The organization of the paper is as follows. A brief description of experimental setup including specimen configurations used for two different mode-I crack tip speeds, a loading setup and a dynamic photoelastic setup is given in Section 2. In Section 3, experimental results for specimens of three different inclined interface orientation angles are presented. Finally, in Section 4, a summary of the results of this study is discussed.

2. Experimental procedures

A novel wedge-loaded plate specimen configuration proposed by Xu et al. [8] is used to produce a single and straight dynamic mode-I crack. Two specimen configurations used in this study to obtain different mode-I crack tip speeds are shown in Fig. 1. The major advantage of dynamic wedge-loading is the fact that it generates a negative non-singular stress, which enhances the crack path stability and prevents branching [19]. These specimens were made out of Homalite-100, which is a brittle birefringent material. Homalite-100 was chosen because its mechanical properties, wave speeds and dynamic fracture behavior have been well-documented in the literature [20]. Some of the physical properties of Homalite-100 are given in Table 1. The wave speeds are measured using ultrasonics while the rest of the properties are taken from the literature. The overall dimensions of the specimens are $475 \times 380 \times 9.5 \text{ mm}^3$. The reason for choosing such large specimen dimensions is to prevent the effect of reflected waves arriving from the free boundaries on both mode-I and mixed mode crack propagation within the range of field of interest. The field of interest considered in this study is a circle with a diameter of 125 mm, as shown in Fig. 2. Three different interfacial angles ($\alpha = 30^\circ, 45^\circ$ and 60°) are considered in this study. To create weak interfacial bond strength, Loctite-384 adhesive is used to bond the interfaces. The

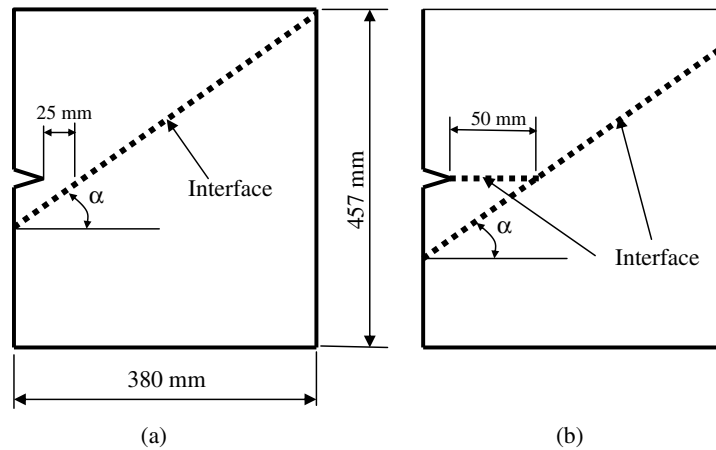


Fig. 1. Specimen configurations.

Table 1
Optical and mechanical properties of Homalite-100 used in this study

Property	Value
Young's modulus E (MPa)	3860
Poisson's ratio ν	0.35
Material fringe constant f_σ (kN/m)	23.6
Dilatational wave speed C_P (km/s)	2.104
Shear wave speed C_S (km/s)	1.2
Density ρ (kg/m ³)	1230

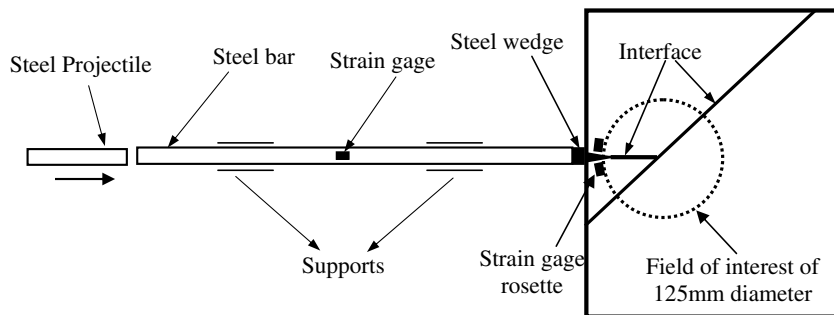


Fig. 2. Modified Hopkinson bar loading setup.

adhesive quasi-static fracture toughness is $0.35 \text{ MPa m}^{1/2}$ when it is used to bond two Homalite-100 plates. The average thickness of the adhesive layer is less than $100 \mu\text{m}$.

In Fig. 1a, the specimen is designed to have mode-I crack propagation in Homalite-100 material with a speed ranging from $0.35C_R$ – $0.4C_R$, i.e. slightly below the crack branching speed. However, in the case of a specimen of Fig. 1b, the cracks can achieve speeds as high as $0.75C_R$ – $0.8C_R$. It can be noticed that two different horizontal crack propagation lengths, 25 mm and 50 mm, are used, respectively, in the Fig. 1a and b. The reason for choosing different horizontal crack propagation lengths in these two specimen configurations is to have almost similar loading conditions when the crack approaches the inclined interface. Since the faster crack propagates at almost twice the speed of the slower crack, the horizontal crack propagation length of Fig. 1b is increased to twice of that of Fig. 1a.

As mentioned in the introduction of this paper, a loading setup based on a modified Hopkinson bar apparatus is used to dynamically load the specimens. The diagram of the loading setup is shown in Fig. 2. The loading setup consists of a steel bar, a steel projectile and a steel wedge. This loading setup provides

well-controlled dynamic loading conditions, which can be monitored by bonding a strain gage onto the Hopkinson bar. A steel wedge is inserted into the notch of the specimen. The specimen with the wedge is held against the bar without any gap. A gas gun is used to impact the Hopkinson bar with a 50 mm long steel projectile. The impact generates a compressive pulse which passes through the bar and wedge. This pulse loads the notch faces of the specimen while passing through the wedge. A set of strain gage rosettes are attached at a distance of 4 mm away from the notch faces. These rosettes record the strain values associated with the loading pulses. Using plane stress conditions, the strain pulses are later analyzed to obtain normal stress and shear stress pulses. Typical normal and shear stress pulses obtained from the strain gage rosettes are shown in Fig. 3. As given in the figure, the range of arrival times of mode-I cracks at the inclined interface is 70–80 μs for all experiments reported in this paper. The variation of normal and shear stresses due to applied dynamic loading within this arrival time range is very small, therefore the comparison of experiments within this time range is acceptable. As reported in Fig. 3, the stress pulses are almost symmetric in all of the experiments reported in this paper.

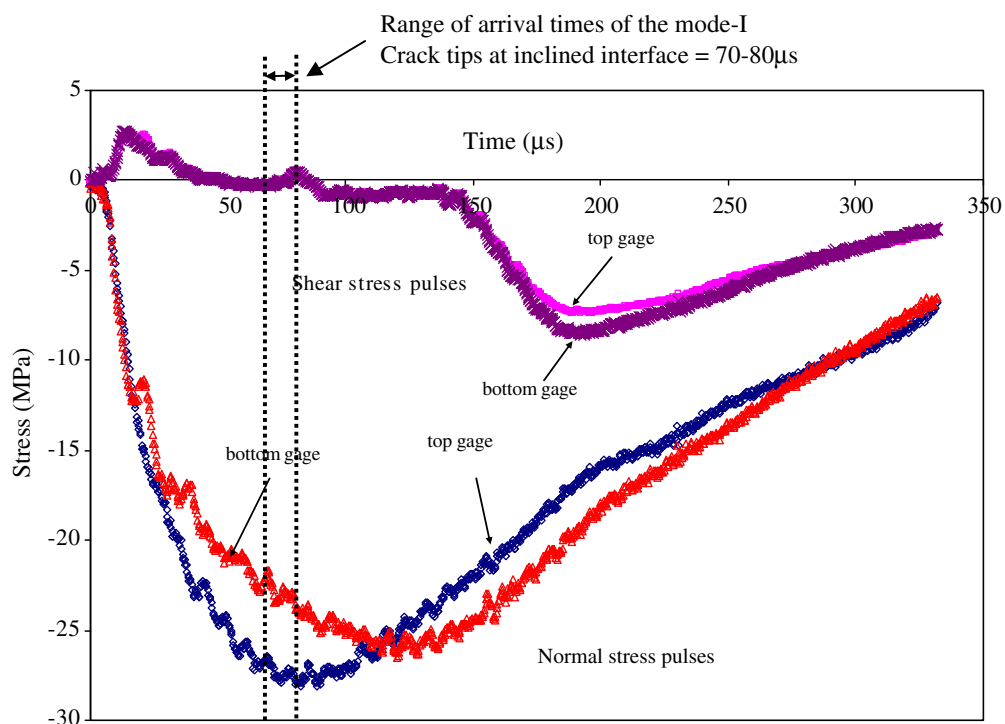


Fig. 3. Typical normal and shear loading pulses.

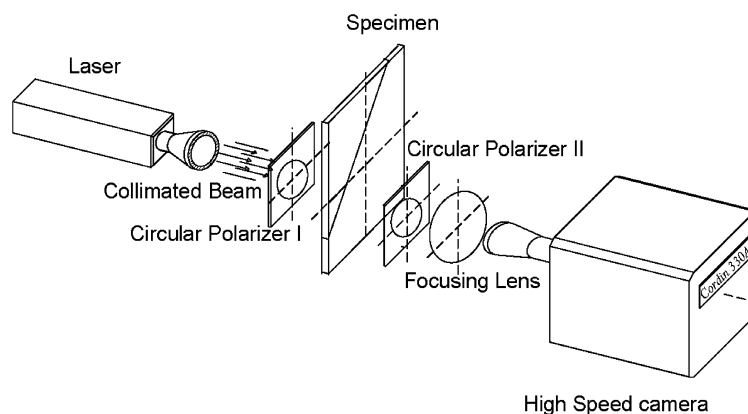


Fig. 4. Dynamic Photoelastic experimental setup.

The other important part of the experimental setup is the dynamic photoelasticity setup as shown in Fig. 4. It consists of a laser light source, a set of circular polarizer sheets, and a high-speed camera. A collimated beam is used to illuminate the specimen, which is sandwiched between the two circular polarizer sheets. The high-speed camera is used to capture the photoelastic fringes associated with a propagating crack. The high-speed camera system is able to capture the images at a framing rate of 100 million frames per second with exposure times as low as 10 ns. In this study, the high-speed camera is operated at a much slower speed, around 0.2–0.4 million frames per second.

3. Experimental observations

As discussed in the introduction, for proper comparison of the results of various specimen configurations with similar loading conditions, a constant projectile speed of 20–22 m/s was chosen. Dynamic photoelasticity in conjunction with high-speed photography provides full-field information in terms of isochromatics of real-time crack propagation. This information provides valid data regarding crack tip position, crack tip velocity and the deflection/penetration behavior of a mode-I crack upon reaching the inclined interface. The following sections discuss these observations for specimens of each inclined interface angle, $\alpha = 30^\circ$, 45° and 60° .

3.1. Specimens of inclined interface angle, $\alpha = 30^\circ$

A set of isochromatic fringe patterns associated with dynamic crack propagation for two specimen configurations of $\alpha = 30^\circ$ is shown in Fig. 5. The time (t) values mentioned in this figure and other figures show-

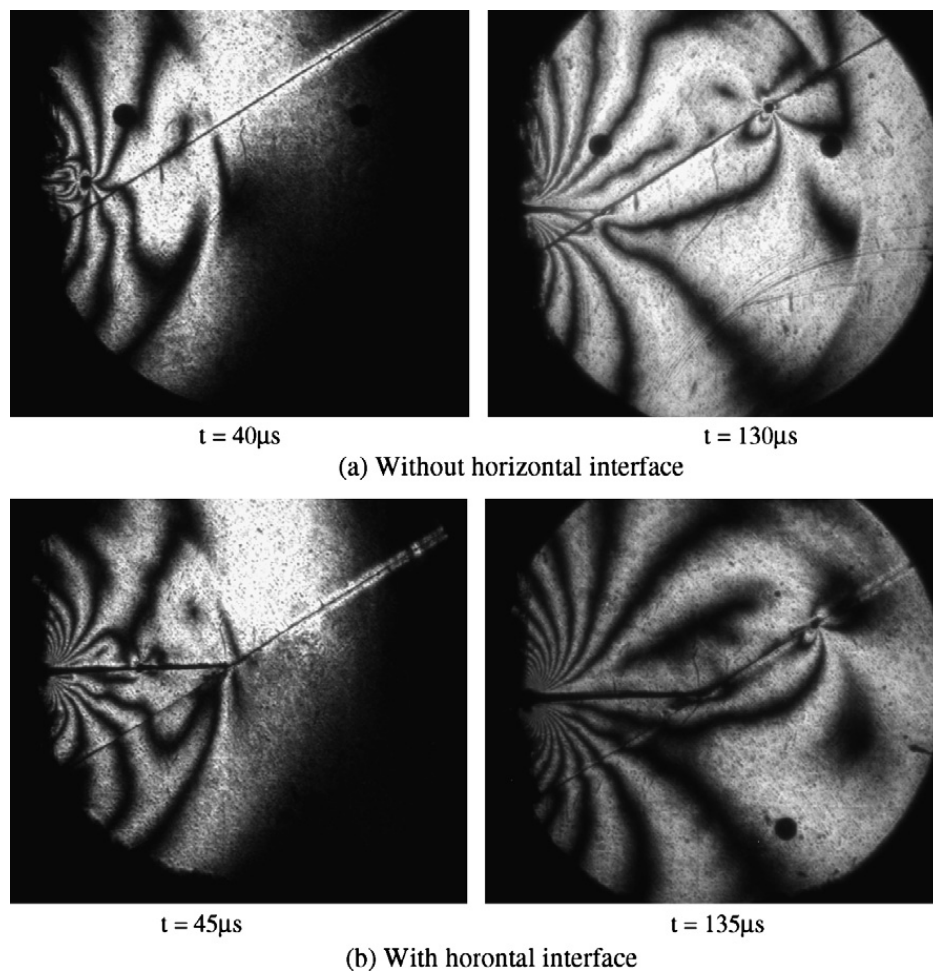


Fig. 5. Isochromatics associated with a propagating crack for an inclined interface, $\alpha = 30^\circ$ (the black circular spot in the figures represents a scale of 6.25 mm).

ing isochromatics in this paper are timing values after the initiation of the dynamic loading on notch faces of the specimen. The black circular spot shown in all figures is a scaling mark of 6.25 mm in diameter. As shown in Fig. 5a, the mode-I crack tip of the specimen ($t = 40 \mu\text{s}$) without horizontal interface can be clearly identified by the bigger shadow spot corresponding to a traveling stress singularity as well as from the increased concentration of focused isochromatics at the crack tip. However, the shadow spot associated with the mode-I crack of the specimen ($t = 45 \mu\text{s}$) corresponding to the horizontal interface shown in Fig. 5b is small due to the fact that the propagating toughness of a weak interface is much smaller compared to the propagating toughness of the Homalite-100. For the specimen in Fig. 5a and b, the mode-I crack reaches the inclined interface at around $70 \mu\text{s}$ and $78 \mu\text{s}$, respectively. For both cases in Fig. 5, the isochromatic fringes associated with propagating cracks along inclined interfaces have a similar pattern except for a small difference in size of the fringes. The asymmetry in fringe patterns of the inclined interfacial cracks represents the existence of mode-mixity.

The crack tip velocity vs. time records for both specimen configurations of $\alpha = 30^\circ$ are shown in Fig. 6. For a specimen without horizontal interface, the mode-I crack propagates at an average velocity of 384 m/s before reaching the inclined interface. However, as reported by Xu et al. [8] the crack jumps to a much higher velocity when it is deflected onto a weak inclined interface. The average crack tip velocity along the inclined interface for this specimen configuration is around 917 m/s. In the case of a specimen with a horizontal interface, for similar loading conditions, the mode-I crack propagates at an average velocity of 720 m/s without any branching. The weak interface or path suppresses any micro-branching while the crack is propagating and lets the crack propagate at much higher mode-I crack speeds than the branching speed of Homalite-100 material. Surprisingly this crack tip does not jump to a much higher speed that is similar to previous specimen configuration after reaching the inclined interface. It propagates with the same average velocity (714 m/s) along the inclined interface. It seems that the mode-I crack, which is propagating along the horizontal interface, has not experienced any change in fracture resistance when deflected to propagate along the inclined interface of $\alpha = 30^\circ$. It can also be noted from the Fig. 6 that the crack slows down when it is propagating along an inclined interface.

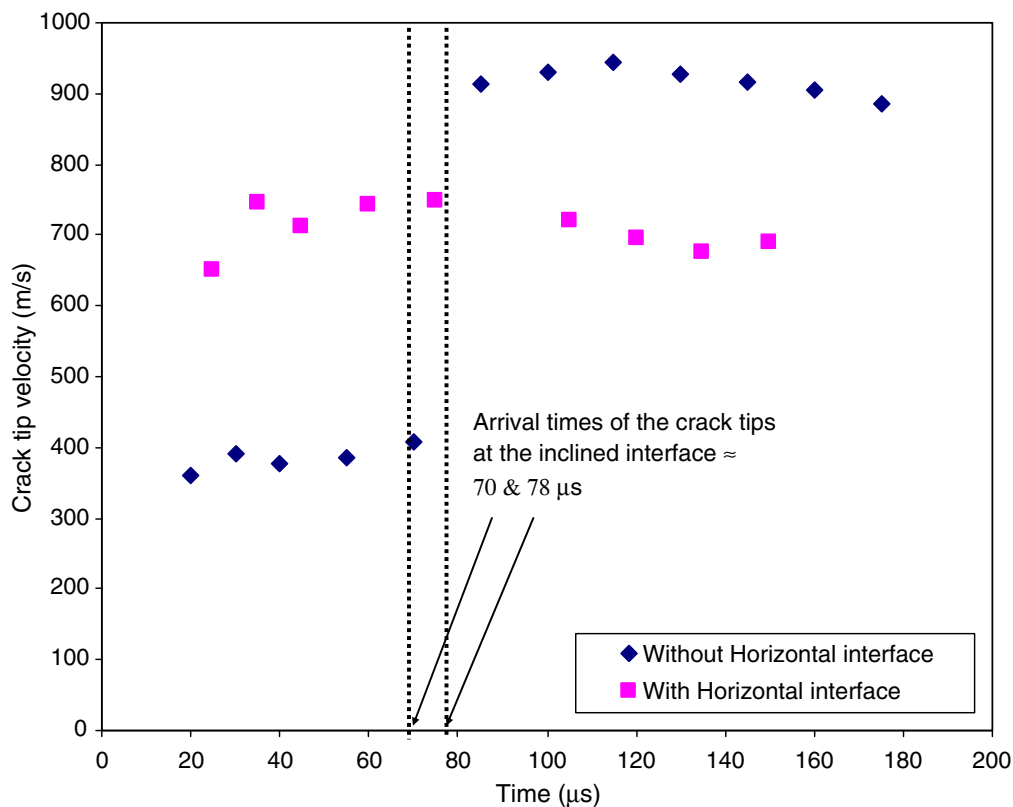


Fig. 6. Crack tip velocity history of a propagating crack for an inclined interface, $\alpha = 30^\circ$.

The reason for this reduction in crack velocity is that as the crack propagates further on the inclined interface, it moves away from loading points, i.e., notch faces.

As shown in Fig. 5a and b, for the frames of $t = 130 \mu\text{s}$ and $t = 135 \mu\text{s}$, respectively, the mode-I crack has clear deflection without any penetration. It is observed for the specimens of other inclination angles that if the crack penetrates while it deflects, it does so approximately at right angle to the inclined interface. As reported by Rosakis et al. [18], when a mixed-mode crack propagates along the weak interface, it generates micro-cracks (along the tensile side of shear) within the process zone of crack tip. These micro-tensile cracks become bigger when the loading conditions are favorable to them. The angle of these tensile cracks is usually dependent on crack tip stress conditions and more importantly non-singular stress or T-stress acting horizontal to the crack line. Therefore for $\alpha = 30^\circ$, the penetration angle of tensile crack would be approximately 60° as shown in Fig. 7a. It seems that the resistance to penetration at this angle is much higher for both mode-I crack tip velocities. This finding is reinforced by the fact that no micro-cracks are observed on the tensile side of the interface for specimens of $\alpha = 30^\circ$. Even the applied impact loading is increased by 50% for specimen configuration with horizontal interface; there are no penetration attempts for inclination angle of $\alpha = 30^\circ$.

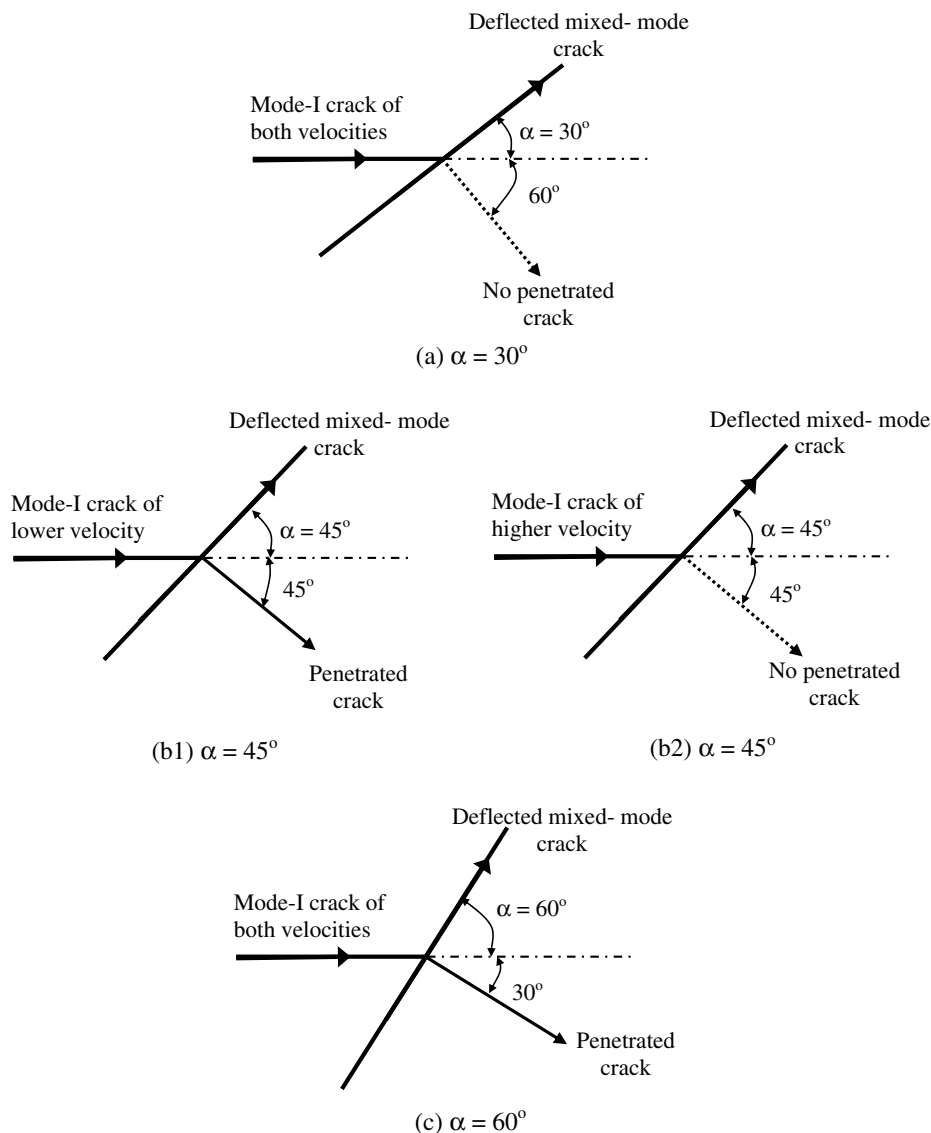


Fig. 7. Schematic diagram showing the deflection/penetration behavior of incoming mode-I crack when it reaches inclined interface.

3.2. Specimens of inclined interface angle, $\alpha = 45^\circ$

Isochromatic fringe patterns associated with dynamic crack propagation for two specimen configurations of $\alpha = 45^\circ$ are shown in Fig. 8. For both cases in Fig. 8, the isochromatic fringes associated with propagating cracks along inclined interfaces have similar patterns except for a small difference in size of the fringes. The high asymmetry in the fringe patterns of the inclined interfacial cracks compared to $\alpha = 30^\circ$ represents the existence of high mode-mixity in this case. The crack tip velocity vs. time records for both specimen configurations of $\alpha = 45^\circ$ are shown in Fig. 9. Again for a specimen without horizontal interface, the mode-I crack propagates at an average velocity of 393 m/s before reaching the inclined interface. The average crack tip velocity along the inclined interface for this specimen configuration is around 841 m/s. It is interesting to note here that for almost the same mode-I crack velocity, keeping in mind the similar loading conditions, the mixed-mode crack propagates at slightly lower velocity compared to that of $\alpha = 30^\circ$, which is about 917 m/s. It represents that the mixed-mode propagating toughness for $\alpha = 45^\circ$ is slightly higher than that for $\alpha = 30^\circ$. In the case of a specimen with horizontal interface, the mode-I crack propagates with an average velocity of 748 m/s and deflects to propagate at an average velocity of 678 m/s. The crack tip experiences a decrease in velocity when it is deflects on an inclined interface. This again might be an increase in the propagating mixed-mode toughness for $\alpha = 45^\circ$ compared to the mode-I propagating toughness.

In the case of a specimen without horizontal interface as shown in Fig. 8a, for the frame $t = 150 \mu\text{s}$, the crack not only deflects but also penetrates. As soon as the mode-I crack arrives on to the inclined interface, it becomes mixed-mode crack and generates tiny micro-cracks within the process region. Then one of these

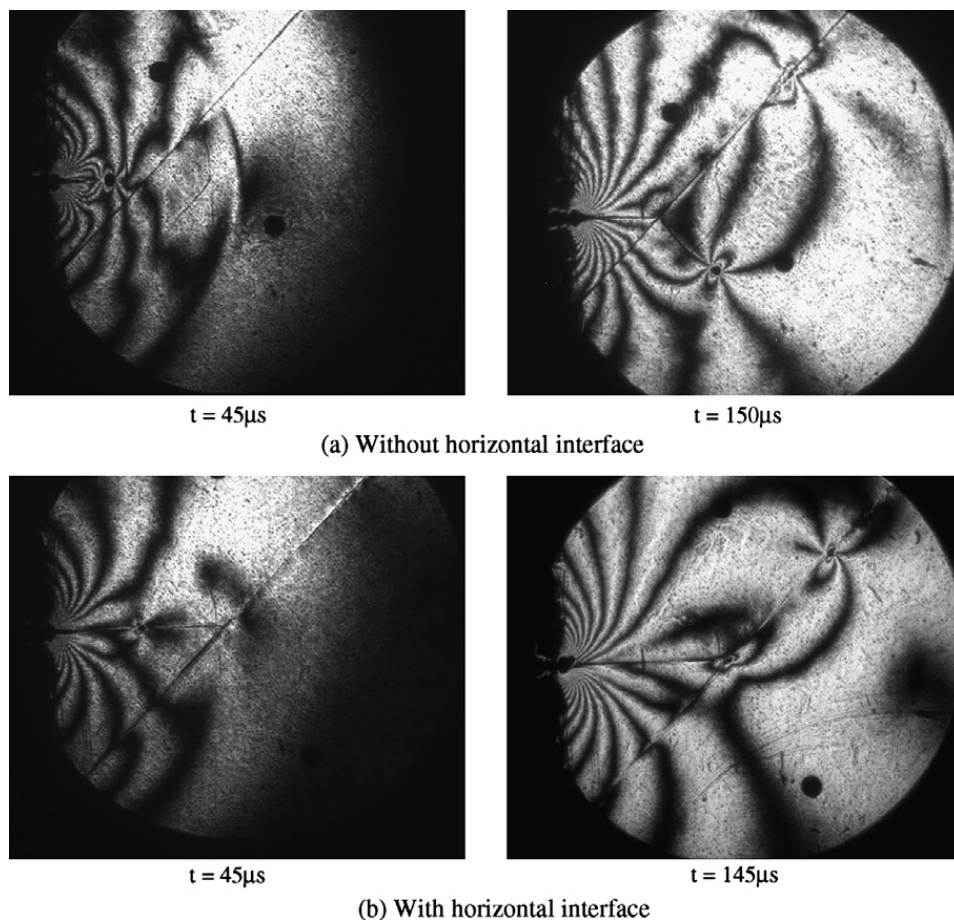


Fig. 8. Isochromatics associated with propagating crack for an inclined interface, $\alpha = 45^\circ$.

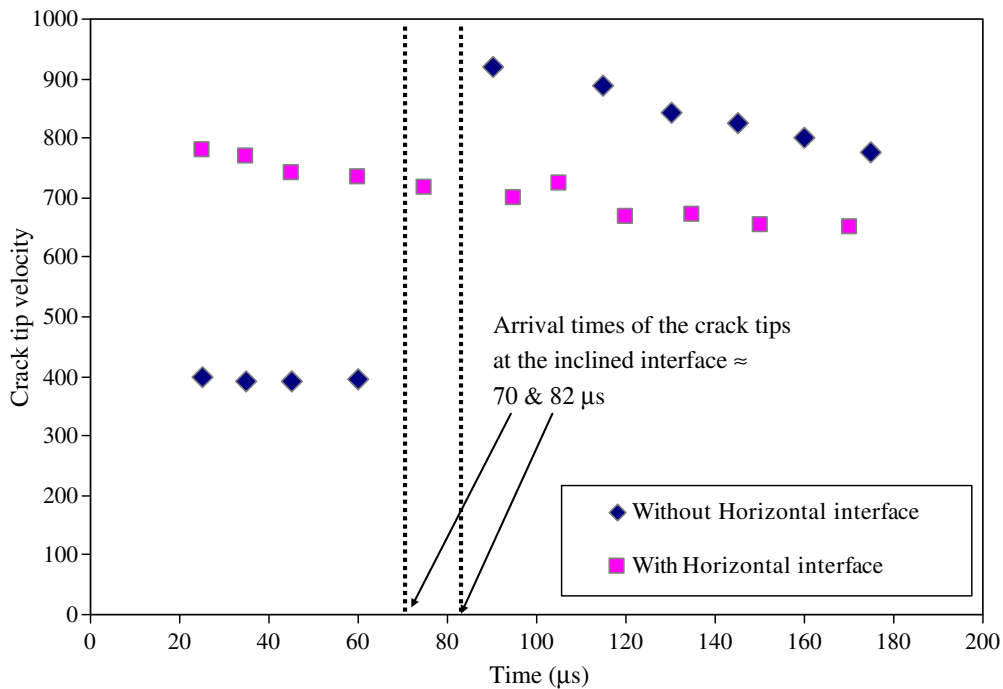


Fig. 9. Crack tip velocity history of a propagating crack for an inclined interface, $\alpha = 45^\circ$.

micro-cracks become a big crack and propagates with very small delay compared to the main deflected crack. The details of the delay of penetrated crack with respect to deflected crack can be seen in the Fig. 10. The penetrated crack propagates with an average velocity of 350 m/s. As we can see from the fringes of the penetrated crack, it propagates with local mode-I conditions with the depiction of symmetric fringes with respect to the penetrated crack line as shown in Fig. 9a. Now for the case of the specimen with horizontal interface as shown in Fig. 8b, the mode-I crack that is coming at an average velocity of 748 m/s only deflects to propagate along an inclined interface without any penetration.

As shown in Fig. 7b1 and b2, if the mode-I crack is willing to penetrate while deflecting along the inclined interface, it needs to turn approximately 45° (favorable tensile direction path) from the incoming mode-I crack direction. It is also understood that the stress-field or energy release associated with the mode-I crack coming at lower velocity (in Homalite-100 material) is much higher than that of a higher velocity (along weak plane). This higher stress-field or energy release rate can overcome the resistance offered by the favorable tensile direc-

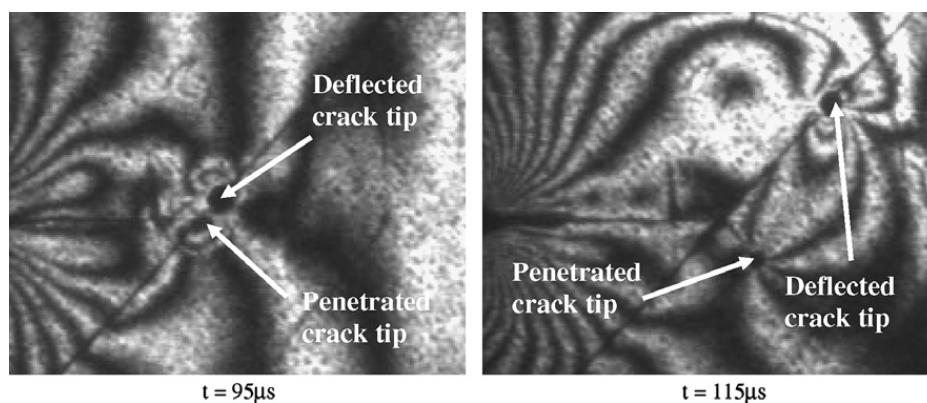


Fig. 10. Sequence of frames showing slight delay of penetrated crack compared to deflected crack for the specimen configuration shown in Fig. 8a.

tion to penetrate, therefore only the specimen without a horizontal interface experiences simultaneous penetration along with deflection.

3.3. Specimens of inclined interface angle, $\alpha = 60^\circ$

A set of isochromatic fringe patterns and crack tip velocity vs. time associated with dynamic crack propagation for two specimen configurations of $\alpha = 60^\circ$ is shown in Figs. 11 and 12, respectively. For a specimen without a horizontal interface, the mode-I crack again propagates at an average velocity of 343 m/s before reaching the inclined interface. The average crack tip velocity along the inclined interface for this specimen configuration is around 668 m/s. Although the incoming mode-I crack tip velocity for this case is slightly lower than that of the other two cases as discussed above, the mixed-mode crack is propagating at a much lower velocity compared to other two cases at $\alpha = 30^\circ$ and 45° . This suggests that the mixed-mode propagation toughness is increasing as the angle of the inclined interface increases. In the case of a specimen with a horizontal interface, the mode-I crack propagates with an average velocity of 673 m/s and deflects to propagate with an average velocity of 592 m/s. Again, there is a considerable decrease in velocity in this mixed-mode crack compared to other two cases, $\alpha = 30^\circ$ and 45° . The summary of the average crack tip velocities of all three cases $\alpha = 30^\circ$, 45° and 60° for two specimen configurations is provided in Table 2.

Both specimen configurations in this case ($\alpha = 60^\circ$) experience simultaneous penetration along with deflection as shown in Fig. 11. As given in the Fig. 7c, the penetrated crack needs to turn approximately

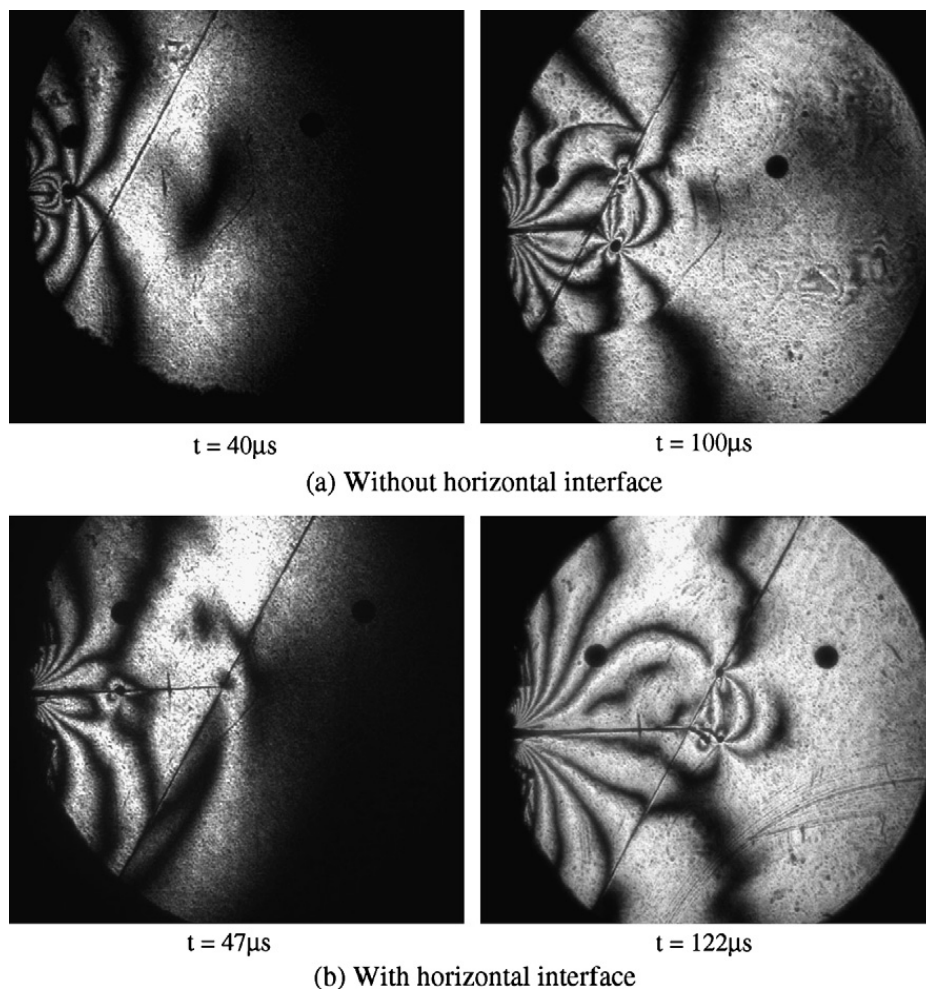


Fig. 11. Isochromatics associated with propagating cracks for an inclined interface, $\alpha = 60^\circ$.

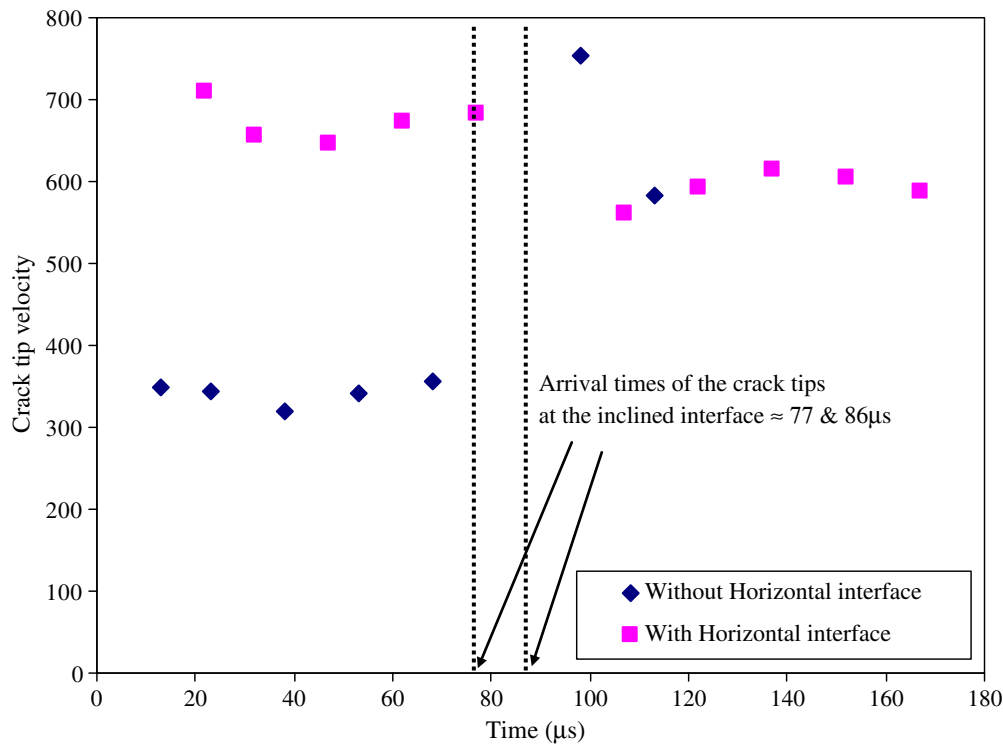


Fig. 12. Crack tip velocity history of a propagating crack for an inclined interface, $\alpha = 60^\circ$.

Table 2
Average velocity (m/s) of crack propagation for all cases

Interface angle	Horizontal interface	Mode-I crack tip velocity (m/s)	Mixed-mode crack tip velocity (m/s)
30°	No	384	917
	Yes	720	714
45°	No	393	841
	Yes	748	678
60°	No	343	668
	Yes	673	592

30° to penetrate in the favorable tensile stress direction. The stress-field or energy release rate associated with the mode-I crack of both velocities matches well with the requirement of resistance of the favorable penetration path, resulting in simultaneous penetration along with deflection in both cases. It is interesting to mention here that the deflected crack of the specimen without a horizontal interface undergoes multiple penetration attempts after having travelled for some distance, as shown in Fig. 11a. The deflected crack eventually penetrates back into the Homalite-100 material. The details of the multiple penetrations and eventual penetration of the deflected crack can be seen in the blow-up picture taken at time $t = 130 \mu\text{s}$ in the Fig. 13a. However, the deflected crack of the specimen with horizontal interface undergoes no penetration attempts during deflection, as shown in Fig. 13b taken at time $t = 152 \mu\text{s}$. The multiple penetration attempts of the first case can be attributed to several reasons. One of the reasons might be that the inclined interface is closer to the loading points of the notch faces in this specimen configuration of $\alpha = 60^\circ$. The closer loading helps to choose favorable tensile paths associated with a propagating mixed-mode stress-field. It is also important to mention here that the penetration angle is no longer perpendicular to the interface. This change in penetration angle is also affected by the closeness of the inclined interface to the loading points of the specimen, as well as the change in non-singular stress (T-stress) associated with the propagating crack.

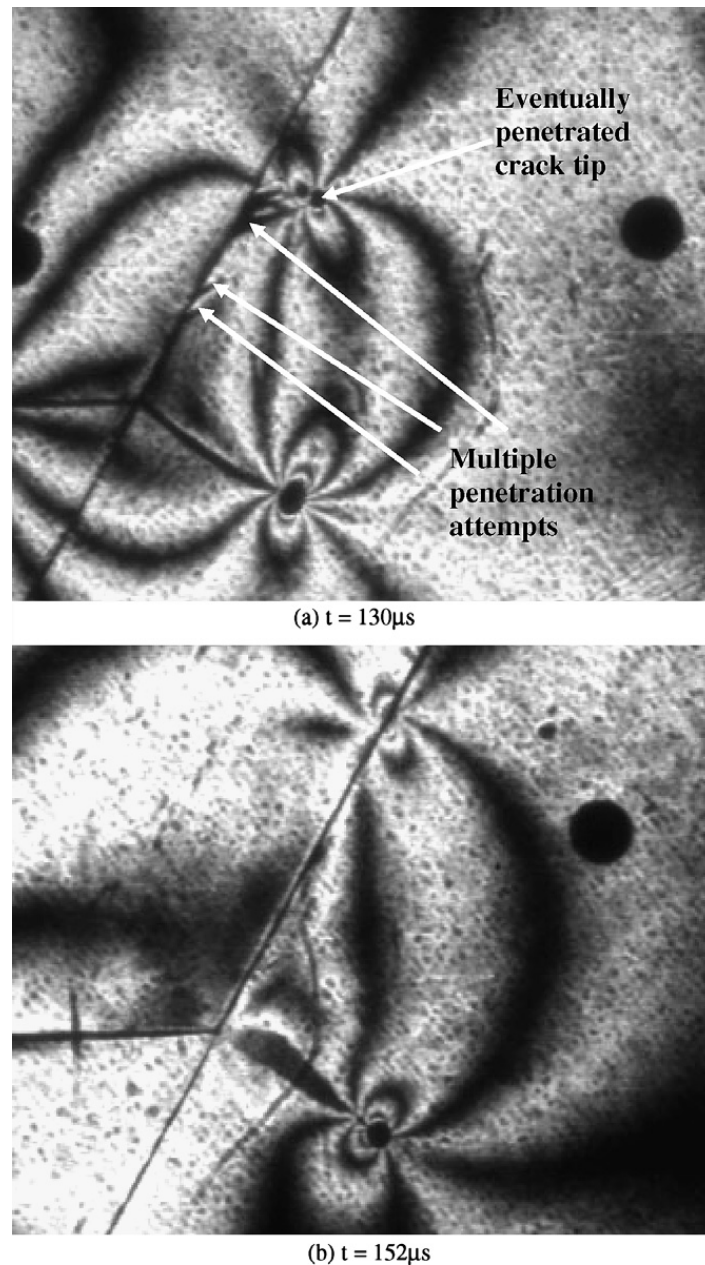


Fig. 13. Details of deflected crack of both specimen configurations for $\alpha = 60^\circ$.

4. Conclusions

An experimental investigation has been performed to understand deflection/penetration behavior for mode-I cracks propagating towards three different inclined interfaces. For slower mode-I cracks, there exists a speed jump as reported by previous studies. However, for higher mode-I crack velocities, cracks deflect and travel with the same speeds without any speed jumps. For similar mode-I crack tip velocities, the deflected mixed-mode crack tip velocities decrease as the angle of inclined interface increases. As the angle of the inclined interface increases, the mode-I cracks undergoes penetration along with deflection since the angle of the most favorable tensile direction decreases. For a specimen without a horizontal interface of $\alpha = 60^\circ$, along with initial penetration, there are multiple penetration attempts and eventual penetration after the deflected crack propagates for a short distance along the inclined interface.

Acknowledgements

The authors would like to acknowledge the support of the Department of Energy through the ASCI-ASAP program, grant number DIM.ASC 1.1.7S LLNL.ASCP. Helpful discussions with Dr. Soonsung Hong and Prof. G. Ravichandran from Caltech are also acknowledged.

References

- [1] Freund LB. *Dynamic fracture mechanics*. New York: Cambridge University Press; 1990.
- [2] Broberg KB. *Cracks and fracture*. San Diego: Academic Press; 1999.
- [3] Washabaugh PG, Knauss WG. A reconciliation of dynamic crack growth velocity and Rayleigh wave speed in isotropic brittle solids. *Int J Fract* 1994;65:97–114.
- [4] Rosakis AJ, Samudrala O, Coker D. Cracks faster than shear wave speed. *Science* 1999;284:1337–40.
- [5] Gao H, Huang Y, Gumbsch P, Rosakis AJ. On radiation-free transonic motion of cracks and dislocations. *J Mech Phys Solids* 1999;47:1941–61.
- [6] Geubelle PH, Kubair D. Intersonic crack propagation in homogeneous media under shear-dominated loading: numerical analysis. *J Mech Phys Solids* 2001;49:571–87.
- [7] Xu LR, Rosakis AJ. An experimental study of impact-induced failure events in homogeneous layered materials using dynamic photoelasticity and high-speed photography. *Opt Lasers Engng* 2003;40:263–88.
- [8] Xu LR, Huang YY, Rosakis AJ. Dynamic crack deflection and penetration at interface in homogeneous materials: experimental studies and model predictions. *J Mech Phys Solids* 2003;51:461–86.
- [9] Cook J, Gordon JE. A mechanism for the control of crack propagation in all brittle systems. *Proc Roy Soc* 1964;282A:508–20.
- [10] He MY, Hutchinson JW. Crack deflection at an interface between dissimilar elastic materials. *Int J Solids Struct* 1989;25:1053–67.
- [11] Gupta V, Argon AS, Suo Z. Crack deflection at an interface between two orthotropic materials 2001;59:s79–87.
- [12] Evans AG, Zok FW. Review the physics and mechanics of fiber-reinforced brittle matrix composites. *J Mater Sci* 1994;29:3857–96.
- [13] Martinez D, Gupta V. Energy criterion for crack deflection at an interface between two orthotropic media. *J Mech Phys Solids* 1994;42(8):1247–71.
- [14] Ahn BK, Curtin WA, Parthasarathy TA, Dutton RE. Criteria for crack deflection/penetration for fiber-reinforced ceramic matrix composites. *Compos Sci Technol* 1998;58:1775–84.
- [15] Leguillon D, Lacroix C, Martin E. Interface debonding ahead of a primary crack. *J Mech Phys Solids* 2000;48:2137–61.
- [16] He MY, Hsueh CH, Becher PF. Deflection versus penetration of a wedge-loaded crack: effects of branch-crack length and penetrated-layer width. *Composites: Part B* 2000;31:299–308.
- [17] Qin QH, Zhang X. Crack deflection at an interface between dissimilar piezoelectric materials. *Int J Fract* 2000;102:355–70.
- [18] Rosakis AJ. Intersonic shear cracks and fault ruptures. *Adv Phys* 2002;51(4):1189–257.
- [19] Cotterell B, Rice JR. Slightly curved or kinked cracks. *Int J Fract* 1980;16(2):155–69.
- [20] Dally JW. Dynamic photoelastic studies of fracture. *Exp Mech* 1979;19:349–61.